NANO LETTERS

Letter

pubs.acs.org/NanoLett

Solution Ionic Strength Engineering As a Generic Strategy to Coat Graphene Oxide (GO) on Various Functional Particles and Its Application in High-Performance Lithium–Sulfur (Li–S) Batteries

Jiepeng Rong,[†] Mingyuan Ge,[†] Xin Fang,[†] and Chongwu Zhou*[,‡]

[†]The Mork Family Department of Chemical Engineering and Materials Science and [‡]Ming Hsieh Department of Electrical Engineering, University of Southern California, Los Angeles, California 90089, United States

Supporting Information

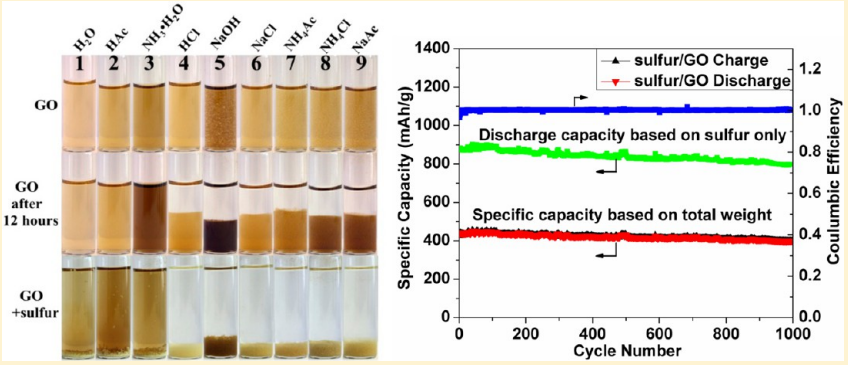

ABSTRACT: A generic and facile method of coating graphene oxide (GO) on particles is reported, with sulfur/GO core–shell particles demonstrated as an example for lithium–sulfur (Li–S) battery application with superior performance. Particles of different diameters (ranging from 100 nm to 10 μm), geometries, and compositions (sulfur, silicon, and carbon) are successfully wrapped up by GO, by engineering the ionic strength in solutions. Importantly, our method does not involve any chemical reaction between GO and the wrapped particles, and therefore, it can be extended to vast kinds of functional particles. The applications of sulfur/GO core–shell particles as Li–S battery cathode materials are further investigated, and the results show that sulfur/GO exhibit significant improvements over bare sulfur particles without coating. Galvanic charge–discharge test using GO/sulfur particles shows a specific capacity of 800 mAh/g is retained after 1000 cycles at 1 A/g current rate if only the mass of sulfur is taken into calculation, and 400 mAh/g if the total mass of sulfur/GO is considered. Most importantly, the capacity decay over 1000 cycles is less than 0.02% per cycle. The coating method developed in this study is facile, robust, and versatile and is expected to have wide range of applications in improving the properties of particle materials.

KEYWORDS: *Graphene oxide, sulfur, lithium–sulfur batteries, coating*

Graphene, a monolayer of carbon atoms tightly packed into a two-dimensional (2D) honeycomb sp^2 carbon lattice, has drawn significant attention recently because of its high surface area, chemical stability, mechanical strength, and flexibility.[1] The unique 2D geometry and excellent properties of graphene and graphene oxide (GO) endow them as one of the most commonly used coating materials to form core–shell structured composites, aiming to improve the performance of the core materials for many kinds of applications, such as lithium-ion battery electrode materials,[2−4] corrosion inhibitor,[5,6] photocatalysts,[7] solar cells,[8] sensors,[9] and drug delivery.[10] Currently, researchers typically utilize surfactants[2] to coat GO onto functional particles, which involves extra steps to determine the right kind of surfactant for each kind of particles, and may suffer from the shortcomings of high cost and complexity, and so on. More importantly, a different chemical route needs to be selected for each kind of particles, considering the different surface chemistry among particles.[2−10] This significantly impedes further development of such core–shell structures toward practical applications. Therefore, a more generic and robust approach that can achieve highly uniform coating of GO on those particles with arbitrary sizes, geometries, and compositions are highly desired. Considering different surface chemistry among particles, such as sulfur, silicon, and carbon, it is natural to seek solutions from physical forces, such as electrostatic forces and surface tension, to achieve the above goal. In particular, the wrapping of graphene oxide on sulfur has stimulated a lot of interest due to the potential use as lithium–sulfur (Li–S) battery cathodes. Li–S batteries are promising candidates to power up electric vehicles because of their high theoretical energy density of 2567 W h

Received: September 11, 2013
Revised: November 26, 2013

   dx.doi.org/10.1021/nl403404v | *Nano Lett.* XXXX, XXX, XXX–XXX

Table 1. Comparison of Ionic Strength of Different 1 M Solutions Used for GO Coating in This Study

	DI water	molecular solutions		ionic solutions					
#	1	2	3	4	5	6	7	8	9
solute	N/A	HAc	$NH_3{\cdot}H_2O$	HCl	NaOH	NaCl	NH_4Ac	NH_4Cl	NaAc
ionic strength	0 M	0.0042 M	~0 M	1 M	~1 M	~1 M	~1 M	~1 M	~1 M
notes	N/A	pK_a = 4.756[47]	pK_a = 9.245[48]	pK_a = −9.3[49]	assuming complete dissociation				

kg^{-1}, which is more than 5 times that of lithium-ion batteries based on traditional insertion compound cathodes.[11−13] Other advantages of Li−S batteries are that elemental sulfur is low cost, low toxic, and abundant. However, the practical application of Li−S batteries is greatly hindered by three major challenges including (1) dissolution of intermediate polysulphide into electrolyte, (2) poor electronic conductivity of sulfur, and (3) large volumetric expansion of sulfur upon lithiation, which result in rapid capacity decay and low Coulombic efficiency.[14−18] Encapsulating sulfur particles with conducting materials, such as graphene oxide,[19,20] can improve their electronic conductivity and limit polysulphide dissolution simultaneously. Significant progress was made by Ji et al.,[19] who coated a layer of sulfur on GO and reported 100 cycles of lithiation and delithiation. However, the sulfur in their work was coated onto GO, instead of being fully wrapped by GO. We note that complete wrapping of graphene oxide on sulfur particles may be the key to mitigate polysulphide dissolution and may reveal itself in improved cycling stability.

In this letter, we report a facile and robust method that is capable of coating GO uniformly on various particles with arbitrary sizes, geometries, and compositions, by engineering the ionic strength in various aqueous solutions. As an example, we have produced sulfur/GO core−shell particles as Li−S battery cathode material showing superior specific capacity of 800 mAh/g after 1000 cycles at 1 A/g current rate if only the mass of sulfur is taken into calculation, and 400 mAh/g if the total mass of sulfur/GO is considered. Most importantly, the capacity decay over 1000 cycles is less than 0.02% per cycle.[14,21] Our method starts with the chemical exfoliation of graphite to prepare GO.[22−31] Although the exact structures of GO are difficult to determine, it is generally believed that GO is rich in epoxides, hydroxyl, keton carbonyls, and carboxylic groups.[32,33] Among those functional groups anchored to GO, it is believed that the carboxylic groups and hydroxyl groups play key roles in helping GO form stable colloids in water.[34−38] Previous studies on the surface charge (zeta potential) of as-prepared GO shows that GO are highly negatively charged when dispersed in water, apparently as a result of ionization of the carboxylic groups and hydroxyl groups that are known to exist on the GO.[29,39,40] The studies suggest that the formation of stable GO colloids is attributed to electrostatic repulsion among adjacent GO.[29] It also implies that positive-charged ions in aqueous solutions can be attracted onto the surface of negatively charged GO, screen the electrostatic repulsion among GO, and eventually disturb the stable dispersion of GO.

Inspired by this deliberation, we chose two categories of solutions with significantly different concentrations of ions, i.e., ionic solutions (also known as "electrolyte") and molecular solutions as dispersing medium to prepare GO suspensions. Ionic strength is widely used to measure the concentrations of ions in solutions, and the ionic strength of used solutions are estimated and compared in Table 1. The ionic strength is around 1 for ionic solutions, which are more than 2 orders of magnitude higher than that of molecular solutions used in our experiments. The difference in ionic strength between ionic solutions and molecular solutions indicates that there are abundant positive and negative charged ions in ionic solutions, while there are much less charged ions in molecular solutions. Different ionic strengths result from the nature of different solute compounds. In ionic solutions, solute compounds dissociate into positively charged cations and negatively charged anions easily, when the ionic bonds holding ions together are broken by polar solvents, such as water. By contrast, in molecular solutions, solute compounds stay as neutral molecules after forming solution. We speculate that the availability of charged ions will make a difference in the dispersion of GO in corresponding solutions. GO was first dispersed in different solutions listed in Table 1, and the results are shown in Figure 1a. When GO is dispersed in deionized

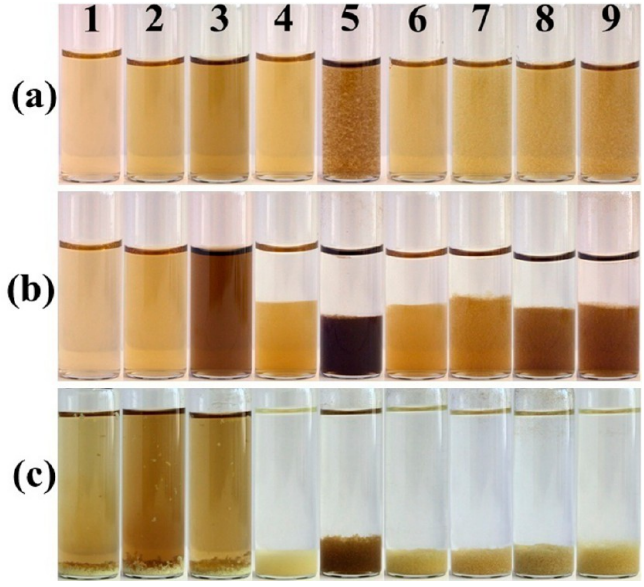

Figure 1. Digital camera images of (a) GO dispersed in different solutions at the beginning. (b) GO dispersion after 12 h and (c) after adding sulfur particles to GO dispersion in panel a. Solutions #1 to #9 are 1 M solutions with solutes #1 to #9 listed in Table 1

(DI) water (#1), it forms stable colloid for days without precipitation. Similar results were observed in molecular solutions, such as #2 (1 M acetic acid (HAc)) and #3 (1 M ammonium hydroxide ($NH_3{\cdot}H_2O$)). In these solutions, the solutes are in the form of molecules after being dissolved in water. Neutrally charged molecules do not have an effect on the electrostatic repulsions among GO, which can still be stable suspension in these solutions. While in ionic solutions, such as #4 (1 M HCl), #5 (1 M NaOH), #6 (1 M NaCl), #7 (NH_4Ac), #8 (1 M NH_4Cl), and #9 (1 M NaAc), the solute compounds are readily dissociated into ions after dissolution. The positive ions will be attracted to and neutralize the negatively charged GO, screen the electrostatic repulsion between GO, and break the stable dispersion of GO. Precipitation of GO was clearly

dx.doi.org/10.1021/nl403404v | Nano Lett. XXXX, XXX, XXX−XXX

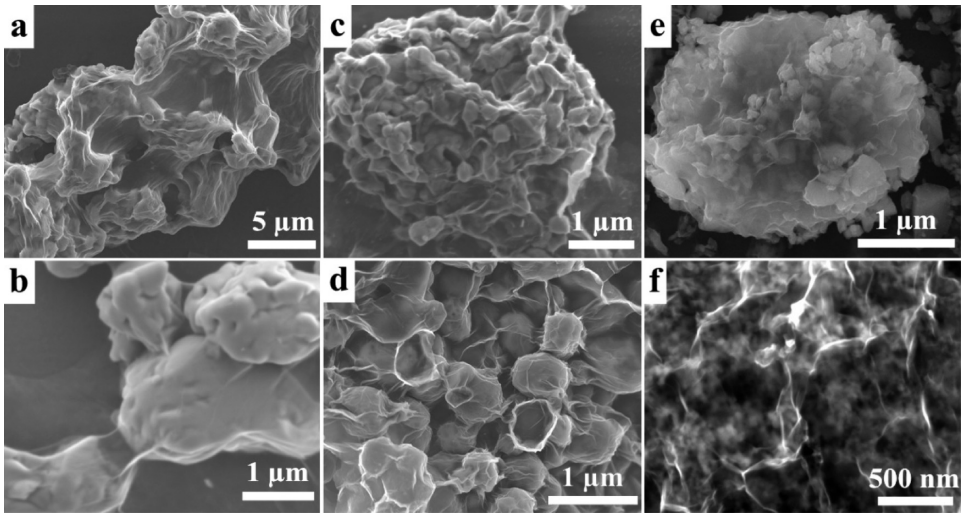

Figure 2. SEM characterization of GO coated onto different particles. (a,b) GO-coated sulfur particles (diameter between 1 and 10 μm). (c,d) GO-coated sulfur particles (diameter ≈ 500 nm). (e) GO-coated ball-milled silicon particles. (f) GO-coated commercial carbon black particles.

observed after 12 h rest in all 6 kinds of ionic solutions (Figure 1b).

GO from both ionic solutions and molecular solutions were dried directly without washing and characterized using scanning electron microscopy (SEM) (Figure S-1, Supporting Information). To minimize the effect of solute compounds on characterization, GO from solution #3 (1 M $NH_3{\cdot}H_2O$) and solution #4 (1 M HCl) are used as examples of each case. As we know, $NH_3{\cdot}H_2O$ and HCl will evaporate away at elevated temperature leaving GO alone. SEM images of GO from ionic solutions showed wrinkled and crumpled morphology. By contrast, GO from molecular solutions exhibited a rather flat surface. The different morphologies of dry GO are attributed to their different dispersion morphologies in solutions. Specifically speaking, after GO was dispersed in ionic solutions, the electrostatic repulsive forces among GO was screened by positively charged ions. GO would tend to crumple and form wrinkles to minimize its surface energy. The morphology of GO is maintained after direct drying. By contrast, GO is stretched out and forms stable dispersion in molecular solutions due to the negatively charged surface. As neutral molecules had no effect on GO, GO remained spread-out on the substrate after drying.

If GO is the only additive into the ionic solutions, they tend to crumple, form wrinkles, and restack to minimize their surface energy as shown in Figure S-1, Supporting Information. When there are other particles existing in ionic solutions, there will be one extra way for GO to minimize the surface energy, which is coating on the particles next to them, losing the inner side of its surface, and forming a core−shell structure. To verify this assumption, sulfur particles in the diameters between 1 and 10 μm, prepared from hand-grounding commercial sulfur powder with pestle and mortar, were used as an example. The particles were added to GO suspensions in solutions #1 to #9. As expected, ionic solutions and molecular solutions showed completely different behaviors. In ionic solutions (#4 to #9), GO precipitated together with sulfur particles, leaving the upper solution transparent. SEM characterization of the sediments confirms that GO with wrinkles conformally coated on all sulfur particles and formed sulfur/GO core−shell structures (Figure 2a,b; see Supporting Information for details). Weight ratios of GO to sulfur in 1:1 (Figure 2a) and 1:5 (Figure 2b) were used in the experiments and complete coating has been achieved in both cases. Simply by adjusting the weight ratio of GO to sulfur, thickness of GO coating can be tuned. It is noted that sulfur particles in very irregular shapes were also coated with GO conformally as shown in Figure 2b. The mechanism of the GO coating on sulfur particles is that GO will lose electrostatic repulsive force in high concentration ionic solutions and take hours to precipitate out because of their low density. During this process, if any particles, such as sulfur particles, exist in the solution, GO will tend to coat on their surface to minimize the surface energy. However, in molecular solutions, sulfur particles precipitate by themselves because of their high density, while GO still uniformly disperses in the solutions as a result of electrostatic repulsion among the negatively charged GO (Figure 1c, solutions #1 to #3).

Because the coating process does not involve any chemical reaction, the method can be extended to other particles with different compositions and sizes. To verify this, the same procedures were applied to three other particles, which were sulfur particles with smaller diameter (diameter ≈ 500 nm, see Supporting Information for synthesis method), ball-milled silicon particles (diameter < 500 nm, see Supporting Information for synthesis method), and commercial carbon black particles (diameter ≈ 100 nm). As expected, each of the three kinds of particles precipitated out with GO coating on their outer surface in the ionic solutions, while the particles sediment by themselves without GO coating in molecular solutions. SEM characterization confirms the complete and uniform wrapping of GO on particles. Figure 2c,d shows the sulfur particles coated with GO in low and high magnifications, respectively. It can be seen that sulfur particles aggregated together, forming clusters in the diameters of a few micrometers, and GO with wrinkles coated on the clusters conformally. Similarly, in Figure 2e,f, silicon-particle aggregates and carbon black aggregates were completely coated with wrinkled GO, respectively.

To study the reaction mechanism and the composition of the products, infrared spectroscopy (IR) and Raman spectroscopy characterization were carried out over GO, bare sulfur particles (diameter = 1 to 10 μm), and sulfur/GO core−shell particles (as shown in Figure 2a; sulfur/GO = 1:1 weight ratio; diameter of sulfur = 1 to 10 μm; solution #4 was used as dispersing

dx.doi.org/10.1021/nl403404v | *Nano Lett.* XXXX, XXX, XXX−XXX

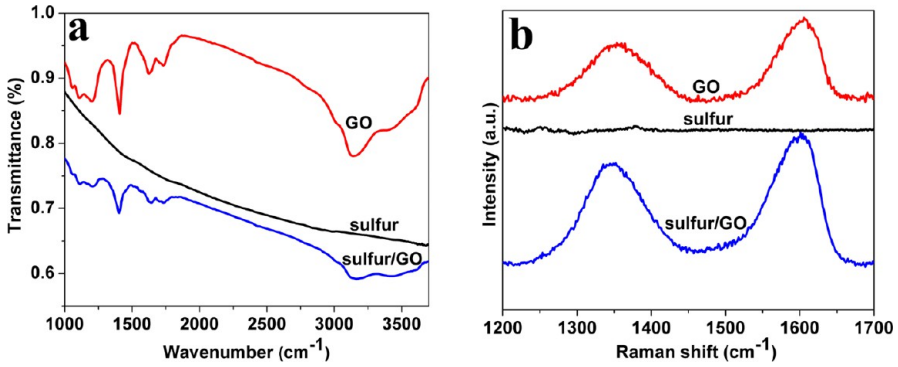

Figure 3. Spectroscopic characterizations. (a) Infrared spectra and (b) Raman spectra of GO, bare sulfur particles, and sulfur/GO core−shell particles. The Raman spectra were taken using a 514 nm laser.

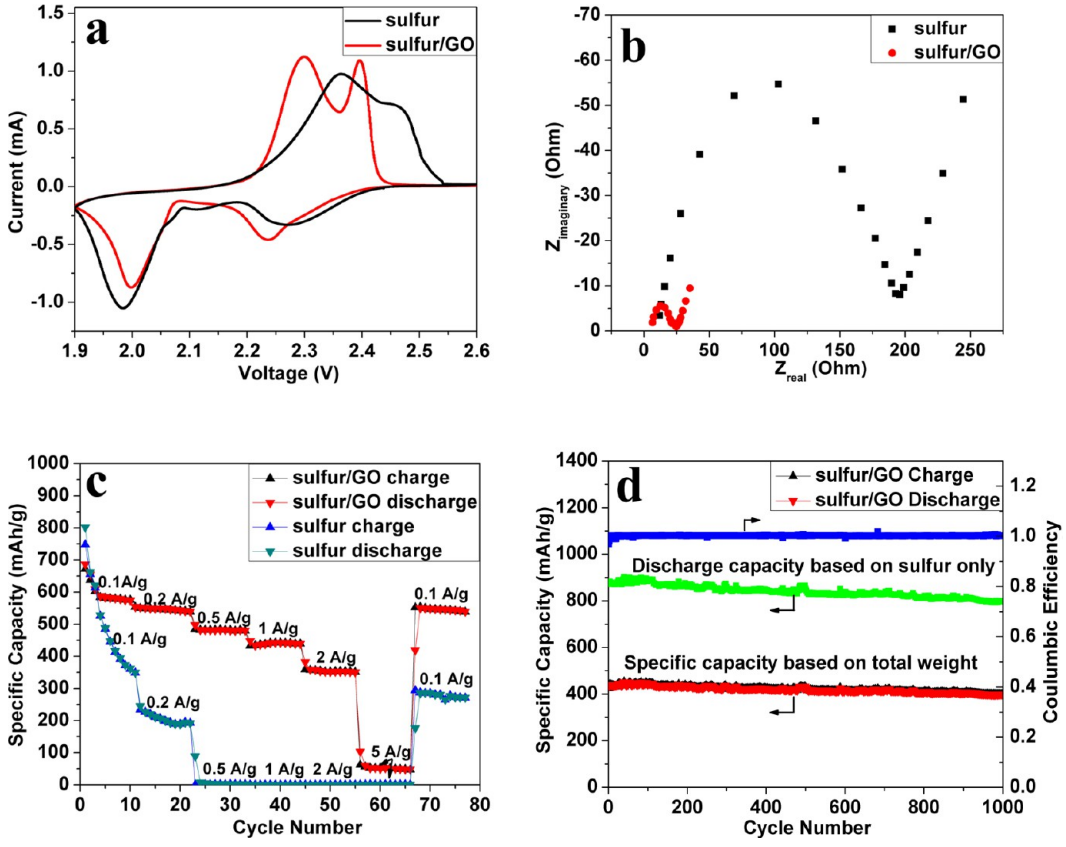

Figure 4. Electrochemical measurements of bare sulfur particles and sulfur/GO core−shell particles as Li−S battery cathode materials. (a) Cyclic voltammetry of sulfur and sulfur/GO at 0.1 mV/s in a potential window from 1.9 to 2.6 V vs Li^+/Li^0. (b) Nyquist plot of impedance measurements of sulfur and sulfur/GO. (c) Specific capacity at different current rates of sulfur and sulfur/GO. (d) Galvanic charge−discharge performance and Coulombic efficiency of sulfur/GO at 1 A/g for 1000 cycles. Discharge specific capacity calculated based on weight of sulfur only (green dotted line) and total weight of sulfur/GO are plotted.

medium in synthesis). In IR spectra (Figure 3a), the following functional groups were identified in GO: O−H stretching vibration (3420 cm^{-1}), C═O stretching vibration (1720−1740 cm^{-1}), C═C from unoxidized sp^2 CC bonds (1590−1620 cm^{-1}), and C−O vibration (1250 cm^{-1}). The results showed good agreement with the literature.[41] The spectrum from bare sulfur showed a rather smooth curve, and no identified signal between 1000 and 3700 cm^{-1}, indicating sulfur has no corresponding functional group on its surface. IR spectrum from sulfur/GO core−shell particles exhibited exactly the same peak positions as that of GO, indicating that all the functional groups from GO remain intact after coating and also confirming the existence of GO in sulfur/GO core−shell particles. This suggests that there were no chemical reactions between GO and sulfur in preparing sulfur/GO core−shell particles. The only driving force leading to GO coating on sulfur particles should be the tendency of lowing surface energy of GO.

To further verify the mechanism of GO coating process, Raman spectroscopy measurements were carried out on GO, bare sulfur particles, and sulfur/GO core−shell particles as well. Raman spectra showed tangential G modes at ∼1590 cm^{-1} and disorder-induced D modes at ∼1350 cm^{-1} from both GO and sulfur/GO, confirming the existence of GO in both samples.

dx.doi.org/10.1021/nl403404v | *Nano Lett.* XXXX, XXX, XXX−XXX

The I_D/I_G ratios of both GO and sulfur/GO were calculated to be around 0.8, indicating that the quality of GO did not change much after coating on sulfur particles. There was no observable peak between 1200 to 1700 cm^{-1} from sulfur or silicon wafer substrate used for all Raman characterizations.

As discussed above, one of the most important applications of sulfur particles is the use as lithium−sulfur (Li−S) battery cathodes. We believe that by using sulfur/GO core−shell particles prepared above (sulfur/GO = 1:1 weight ratio; see Supporting Information for TGA measurement; diameter of sulfur =1 to 10 μm, as shown in Figure 2a; solution #4 was used as dispersing medium in synthesis) as cathode material in Li−S batteries, the three major challenges faced by sulfur cathode can be tackled simultaneously. GO coating can improve electronic conductivity and limit polysulphide dissolution, and rich wrinkles in GO can provide extra space for volume expansion of sulfur upon lithiation and prevent the electrode from disruption.

In order to demonstrate the structural benefits of sulfur/GO core−shell particles in improving cathode performance, a series of electrochemical measurements were carried out. As a comparison, bare sulfur particles (denoted as sulfur in Figure 4) without GO was also tested following the same procedures. Cyclic voltammetry (CV) was used to reveal the electrochemical reaction mechanism of the cathode materials between 1.9 and 2.6 V at a sweep rate of 0.1 mV/s (Figure 4a). During the first cathodic reduction process of sulfur, two peaks at 2.24 and 2.0 V (vs Li^+/Li^0) were observed. The peak at 2.24 V corresponds to the reduction of sulfur to higher-order polysulfides (Li_2S_x, $4 < x < 8$),[42] while the peak at 2.0 V can be assigned to the reduction of higher-order polysulphides to lower-order polysulphides (Li_2S_x, $2 \leq x \leq 4$).[19,43] In the following anodic oxidation process, two peaks at approximately 2.3 and 2.4 V were observed and can be attributed to the conversion of lithium sulfides to polysulphides and sulfur.[2,44,45] Sulfur/GO core−shell particles also have four corresponding peaks, however, at slightly shifted positions. The two anodic peaks were shifted to lower voltage by 0.07 V, while the two cathodic peaks had much smaller shift. The voltage difference between charge and discharge plateaus of sulfur/GO was overall much smaller than that of sulfur, indicating that GO coating can help to reduce the polarization and inner resistance of the batteries. Lower polarization and inner resistance are key factors to achieve long-cycle stability and high power density in batteries and to improve their overall performance. It is noted that the high voltage peak in cathodic branch shifted to low voltage by 0.05 V after GO coating, which cannot be explained by the theory above. We suspect it is a side effect of a trace amount of moisture in the sulfur/GO sample, and the mechanism deserves further study.

To further support the structural benefits of sulfur/GO core−shell particles comparing to sulfur, electrochemical impedance analyses were conducted on both battery cells from 100 kHz to 10 mHz. The impedance of the cathode in the Li−S batteries depends strongly on the lithium content inside the electrode materials. To maintain uniformity, electrochemical impedance spectroscopy measurements were carried out on the working electrodes at the delithiated state after the first cycle. The Nyquist plots obtained are shown in Figure 4b. The high frequency corresponds to the ohmic serial resistance R_s, which includes both the sheet resistance of the electrode and the resistance of the electrolytes. The semicircle in the middle frequency range indicates the charge transfer resistance R_{ct}, relating to the charge transfer through the electrode/electrolyte interface and the double layer capacity C_{dl} formed due to the electrostatic charge separation near the electrode/electrolyte interface. Also, the inclined line in the low frequency represents the Warburg impedance W_o, which is related to solid-state diffusion of lithium-ions into the electrode material. Sulfur/GO core−shell particles clearly showed a significantly smaller semicircle than sulfur does, and the charge transfer resistance was reduced from 200 Ω for the sulfur sample to 25 Ω for the sulfur/GO sample. In addition, the serial resistance also reduced from 12 to 6.5 Ω after GO coating, indicating a better electrical conductivity of the electrodes. Decreased charge transfer resistance and serial resistance are both favorable to achieve high current rate performance.

In order to demonstrate the improved electrochemical performance of sulfur/GO core−shell particles when it works as a cathode material in Li−S battery, galvanic current measurements were carried out on both sulfur/GO and sulfur at different current rates, as shown in Figure 4c. Sulfur/GO has slightly lower specific capacity in the first three cycles than that of sulfur, owing to the fact that the weight of GO is taken into calculation, but it does not contribute too much capacity. After 10 cycles at 0.1 A/g current rate, specific capacity approaches 600 mAh/g for sulfur/GO, and the corresponding Coulombic efficiency is over 99%. In comparison, the specific capacity is only 350 mAh/g for sulfur under the same test conditions. The improvement in cycling stability of sulfur/GO was more significant as the current rate increases, as shown in Figure 4c. Sulfur/GO showed capacities of 550, 500, 450, 350, and 50 mAh/g at the current rates of 0.2, 0.5, 1, 2, and 5 A/g, respectively. By contrast, sulfur only exhibits 200 mAh/g at the current rates of 0.2 A/g, and negligible values at all higher current rates tested. Moreover, sulfur/GO recovers most of the original capacity when the cycling current is restored to 0.1 A/g, implying that the structure of sulfur/GO electrode remained stable even under high rate cycling. The enhanced cycling stability and high-rate performance can be attributed to the unique structure of conformal coating of the wrinkled GO on sulfur. Corresponding voltage profiles at different current rates for both pure sulfur and sulfur/GO can be found in the Supporting Information (Figure S-3). Further galvanic current tests continued from rate capability tests demonstrate that sulfur/GO maintains a capacity as high as 400 mAh/g at 1 A/g over 1000 cycles when the total mass of sulfur/GO is taken into calculation (Figure 4d). Specific capacity based on the weight of sulfur only is calculated to be around 800 mAh/g after 1000 cycles, which is over 6 times larger than that of commercial metal oxide cathode materials (e.g., $LiCoO_2$ = 120 mAh/g). Voltage profile of selected cycles (1st, 100th, 500th, and 1000th) can be found in Figure S-4 in the Supporting Information. It should be noted that the Coulombic efficiency was mostly above 99.5% after the first three cycles. Most importantly, the sulfur/GO cathode showed only less than 0.02% specific capacity degradation per cycle over 1000 cycles.[14,21] Galvanic current test at low current rate (50 mA/g) was also carried out and showed good stability over 23 cycles (Figure S-5, Supporting Information). We attribute the improved performance to complete wrapping of GO over sulfur particles achieved by engineering the ionic strength of solutions. We believe the spacing between stacked GO layers can be used as channels for lithium ion transportation, but the small spacing would significantly slow down polysulphide dissolution thus leading to excellent cycling stability. That is

dx.doi.org/10.1021/nl403404v | Nano Lett. XXXX, XXX, XXX−XXX

why we still see small but nonzero capacity decay over long cycles. Further improvement in cyclability and rate capability by combining the method developed here with other strategies such as conductive polymer coating[11,46] and pore confinement[11] is ongoing in our lab.

In conclusion, a generic method of coating graphene oxide (GO) on particles by engineering the ionic strength of solutions was developed. Uniform coating of GO on various particles with a wide range of sizes, geometries, and compositions are achieved. This method provides a facile, robust, and generic solution to coat wrinkled GO on different particles in aqueous solution medium. As an example, the application in coating GO on sulfur particles to form sulfur/GO core−shell particles as Li−S battery cathode materials was investigated, and we found that the sulfur/GO composite material exhibits significant improvements in electrochemical performance over sulfur particles without coating. Galvanic charge−discharge test using GO/sulfur particles shows a specific capacity of 800 mAh/g is retained after 1000 cycles at 1 A/g current rate if only the mass of sulfur is taken into calculation and 400 mAh/g if the total mass of sulfur/GO is considered. Most importantly, the sulfur/GO cathode showed only less than 0.02% specific capacity degradation per cycle over 1000 cycles. The coating method is expected to have wide applications in improving the properties of functional particle materials with many other interesting applications.

■ ASSOCIATED CONTENT

Supporting Information

Additional information for methods used for materials preparation and electrochemical measurement (e.g., self-discharge test). This material is available free of charge via the Internet at http://pubs.acs.org.

■ AUTHOR INFORMATION

Corresponding Author

*(C.Z.) E-mail: chongwuz@usc.edu.

Notes

The authors declare no competing financial interest.

■ ACKNOWLEDGMENTS

We acknowledge the University of Southern California for financial support.

■ REFERENCES

(1) Geim, A. K.; Novoselov, K. S. *Nat. Mater.* **2007**, *6*, 183.
(2) Wang, H.; Yang, Y.; Liang, Y.; Robinson, J. T.; Li, Y.; Jackson, A.; Cui, Y.; Dai, H. *Nano Lett.* **2011**, *11*, 2644.
(3) Hu, L.-H.; Wu, F.-Y.; Lin, C.-T.; Khlobystov, A. N.; Li, L.-J. *Nat. Commun.* **2013**, *4*, 1687.
(4) Fang, X.; Ge, M.; Rong, J.; Zhou, C. *J. Mater. Chem. A* **2013**, *1*, 4083.
(5) Dennis, R. V.; Viyannalage, L. T.; Gaikwad, A. V.; Rout, T. K.; Banerjee, S. *Am. Ceram. Soc. Bull.* **2013**, *92*, 18.
(6) Krishnamurthy, A.; Gadhamshetty, V.; Mukherjee, R.; Chen, Z.; Ren, W.; Cheng, H. M.; Koratkar, N. *Carbon* **2013**, *56*, 45.
(7) Khalid, N. R.; Ahmed, E.; Hong, Z.; Ahmad, M.; Zhang, Y.; Khalid, S. *Ceram. Int.* **2013**, *39*, 7107.
(8) Neo, C. Y.; Ouyang, J. *J. Power Sources* **2013**, *222*, 161.
(9) Zeng, Y.; Zhou, Y.; Kong, L.; Zhou, T.; Shi, G. *Biosens. Bioelectron.* **2013**, *45*, 25.
(10) Wang, Y.; Wang, K.; Zhao, J.; Liu, X.; Bu, J.; Yan, X.; Huang, R. *J. Am. Chem. Soc.* **2013**, *135*, 4799.
(11) Ji, X.; Lee, K. T.; Nazar, L. F. *Nat. Mater.* **2009**, *8*, 500.
(12) Ellis, B. L.; Lee, K. T.; Nazar, L. F. *Chem. Mater.* **2010**, *22*, 691.
(13) Bruce, P. G.; Freunberger, S. A.; Hardwick, L. J.; Tarascon, J.-M. *Nat. Mater.* **2012**, *11*, 19.
(14) Seh, Z. W.; Li, W.; Cha, J. J.; Zheng, G.; Yang, Y.; McDowell, M. T.; Hsu, P.-C.; Cui, Y. *Nat. Commun.* **2013**, *4*, 1331.
(15) Mikhaylik, Y. V.; Akridge, J. R. *J. Electrochem. Soc.* **2004**, *151*, A1969.
(16) Yamin, H.; Gorenshtein, A.; Penciner, J.; Sternberg, Y.; Peled, E. *J. Electrochem. Soc.* **1988**, *135*, 1045.
(17) Barchasz, C.; Lepretre, J.-C.; Alloin, F.; Patoux, S. *J. Power Sources* **2012**, *199*, 322.
(18) Aurbach, D.; Pollak, E.; Elazari, R.; Salitra, G.; Kelley, C. S.; Affinito, J. *J. Electrochem. Soc.* **2009**, *156*, A694.
(19) Ji, L.; Rao, M.; Zheng, H.; Zhang, L.; Li, Y.; Duan, W.; Guo, J.; Cairns, E. J.; Zhang, Y. *J. Am. Chem. Soc.* **2011**, *133*, 18522.
(20) Wang, H.; Yang, Y.; Liang, Y.; Robinson, J. T.; Li, Y.; Jackson, A.; Cui, Y.; Dai, H. *Nano Lett.* **2011**, *11*, 2644.
(21) Lu, S.; Cheng, Y.; Wu, X.; Liu, J. *Nano Lett.* **2013**, *13*, 2485.
(22) Ruoff, R. *Nat. Nanotechnol.* **2008**, *3*, 10.
(23) Schniepp, H. C.; Li, J. L.; McAllister, M. J.; Sai, H.; Herrera-Alonso, M.; Adamson, D. H.; Prud'homme, R. K.; Car, R.; Saville, D. A.; Aksay, I. A. *J. Phys. Chem. B* **2006**, *110*, 8535.
(24) Si, Y.; Samulski, E. T. *Nano Lett.* **2008**, *8*, 1679.
(25) Lomeda, J. R.; Doyle, C. D.; Kosynkin, D. V.; Hwang, W.-F.; Tour, J. M. *J. Am. Chem. Soc.* **2008**, *130*, 16201.
(26) Behabtu, N.; Lomeda, J. R.; Green, M. J.; Higginbotham, A. L.; Sinitskii, A.; Kosynkin, D. V.; Tsentalovich, D.; Parra-Vasquez, A. N. G.; Schmidt, J.; Kesselman, E.; Cohen, Y.; Talmon, Y.; Tour, J. M.; Pasquali, M. *Nat. Nanotechnol.* **2010**, *5*, 406.
(27) Stankovich, S.; Dikin, D. A.; Piner, R. D.; Kohlhaas, K. A.; Kleinhammes, A.; Jia, Y.; Wu, Y.; Nguyen, S. T.; Ruoff, R. S. *Carbon* **2007**, *45*, 1558.
(28) Xu, Y.; Bai, H.; Lu, G.; Li, C.; Shi, G. *J. Am. Chem. Soc.* **2008**, *130*, 5856.
(29) Li, D.; Muller, M. B.; Gilje, S.; Kaner, R. B.; Wallace, G. G. *Nat. Nanotechnol.* **2008**, *3*, 101.
(30) Lotya, M.; Hernandez, Y.; King, P. J.; Smith, R. J.; Nicolosi, V.; Karlsson, L. S.; Blighe, F. M.; De, S.; Wang, Z.; McGovern, I. T.; Duesberg, G. S.; Coleman, J. N. *J. Am. Chem. Soc.* **2009**, *131*, 3611.
(31) Dreyer, D. R.; Park, S.; Bielawski, C. W.; Ruoff, R. S. *Chem. Soc. Rev.* **2010**, *39*, 228.
(32) He, H. Y.; Klinowski, J.; Forster, M.; Lerf, A. *Chem. Phys. Lett.* **1998**, *287*, 53.
(33) Stankovich, S.; Piner, R. D.; Chen, X. Q.; Wu, N. Q.; Nguyen, S. T.; Ruoff, R. S. *J. Mater. Chem.* **2006**, *16*, 155.
(34) Kotov, N. A.; Dékány, I.; Fendler, J. H. *Adv. Mater.* **1996**, *8*, 637.
(35) Cassagneau, T.; Guérin, F.; Fendler, J. H. *Langmuir* **2000**, *16*, 7318.
(36) Kovtyukhova, N. I.; Ollivier, P. J.; Martin, B. R.; Mallouk, T. E.; Chizhik, S. A.; Buzaneva, E. V.; Gorchinskiy, A. D. *Chem. Mater.* **1999**, *11*, 771.
(37) Hirata, M.; Gotou, T.; Ohba, M. *Carbon* **2005**, *43*, 503.
(38) Szabó, T.; Szeri, A.; Dékány, I. *Carbon* **2005**, *43*, 87.
(39) Lerf, A.; He, H.; Forster, M.; Klinowski, J. *J. Phys. Chem. B* **1998**, *102*, 4477.
(40) Szabó, T.; Berkesi, O.; Forgó, P.; Josepovits, K.; Sanakis, Y.; Petridis, D.; Dékány, I. *Chem. Mater.* **2006**, *18*, 2740.
(41) Marcano, D. C.; Kosynkin, D. V.; Berlin, J. M.; Sinitskii, A.; Sun, Z. Z.; Slesarev, A.; Alemany, L. B.; Lu, W.; Tour, J. M. *ACS Nano* **2010**, *4*, 4806.
(42) Xiao, L.; Cao, Y.; Xiao, J.; Schwenzer, B.; Engelhard, M. H.; Saraf, L. V.; Nie, Z.; Exarhos, G. J.; Liu, J. *Adv. Mater.* **2012**, *24*, 1176.
(43) Zhou, G.; Wang, D.-W.; Li, F.; Hou, P.-X.; Yin, L.; Liu, C.; Lu, G. Q.; Gentle, I. R.; Cheng, H.-M. *Energy Environ. Sci.* **2012**, *5*, 8901.
(44) Guo, J.; Xu, Y.; Wang, C. *Nano Lett.* **2011**, *11*, 4288.
(45) Zheng, G.; Yang, Y.; Cha, J. J.; Hong, S. S.; Cui, Y. *Nano Lett.* **2011**, *11*, 4462.
(46) Yang, Y.; Yu, G.; Cha, J. J.; Wu, H.; Vosgueritchian, M.; Yao, Y.; Bao, Z.; Cui, Y. *ACS Nano* **2011**, *5*, 9187.

(47) Pauling, L. *The Nature of the Chemical Bond and the Structure of Molecules and Crystals: An Introduction to Modern Structural Chemistry*; Cornell University Press: Ithaca, NY, 1960.
(48) Goldberg, R. N.; Kishore, N.; Lennen, R. M. *J. Phys. Chem. Ref. Data* **2002**, *31*, 231.
(49) Dasent, W. E. *Inorganic Energetics: An Introduction*, 2nd ed; Cambridge University Press: Cambridge, U.K., 1982.

dx.doi.org/10.1021/nl403404v | *Nano Lett.* XXXX, XXX, XXX−XXX